



Optimization of the process for converting *Saba Senegalensis* hulls into biosorbents

Gouledéhi S.G.¹ *, Kouadio D. L.¹, Yapi Y. H. A.¹, Dalogo K.A. P.¹,
Akéssé D. P. V.¹ Dibi B.¹

¹Jean Lorougnon Guédé University, Daloa, Côte d'Ivoire

*Corresponding author, Email address: gillesgouledéhi@ujlg.edu.ci

Received 02 Jan 2025,

Revised 21 Feb 2025,

Accepted 23 Feb 2025

Citation: Gouledéhi S.G.,
Kouadio D.L., Yapi Y.H.A.,
Dalogo.K.A.P., Akéssé
D.P.V., Dibi B. (2025)
*Optimisation of the process
for converting Saba
Senegalensis hulls into
biosorbents, J. Mater.
Environ. Sci., 16(2), 354-370*

Abstract: The textile industry in general, and the craft textile dyeing sector in particular, require large volumes of water and produce considerable quantities of coloured effluents. The aim of this study is to optimize the performance of a biosorbent derived from *Saba Senegalensis* hulls, in the context of waste recovery and water treatment. The performance index used in this study is the methylene blue elimination rate. Optimal conditions were determined using experimental design methodology. To this end, a Plackett-Burman design and a full factorial design (2³) were applied to the screening of six factors, namely: drying temperature (X1), particle size (X2), nature of the activating agent (X3), activation time (X4), concentration of the activating agent (X5) and activation time (X6). Subsequently, a central composite design was adopted for modelling and optimizing the response. A mathematical model based on response surface methodology was established for this purpose. The optimum conditions for preparing the biosorbent were obtained using biomass dried at 60°C, with sizes between 0.2 mm and 0.5 mm, activated with 1 N sulphuric acid at room temperature for 8 h. Under these conditions, a 96.02% removal rate was achieved.

Keywords: *Biosorbent; Saba Senegalensis; Experimental design; Elimination rate; Methylene blue*

1. Introduction

Dyes, which are aromatic organic compounds with a complex structure and are soluble in water, have a significant impact on the aquatic environment. Every year, the dye industry produces around 700,000 tonnes of these compounds (Adegoke and Bello, 2015). Unfortunately, industrial effluents contain a substantial quantity of toxic dyes, which are often discharged into water resources. Approximately 2% of all dyes in the environment enter waterways by various means, contributing to freshwater pollution (Shelke *et al.*, 2022; Akartasse *et al.*, 2022). In this respect, even a minimal concentration of dye in water can cause colouration that is harmful to aquatic life (Katheresan *et al.*, 2018; Aaddouz *et al.*, 2023).

To counter this problem, numerous technologies have been developed to effectively remove dyes from the aquatic environment. These include advanced oxidation (Bilińska and Gmurek, 2021; Chin *et al.*, 2022), catalytic ozonation (Khamparia and Jaspal, 2017), coagulation and flocculation (Verma *et al.*, 2012), electrocoagulation and Fenton oxidation (Thakur and Chauhan, 2018; Jaafar *et al.*, 2016), membrane separation (Moradihamedani, 2022), ion exchange (Hassan *et al.*, 2020) and photocatalysis (Hasanpour and Hatami, 2020; Saeed *et al.*, 2022). However, these technologies have a number of limitations, including the production of toxic sludge, handling and disposal difficulties, the complexity of scale-up, increased effluent colour, high energy consumption, economic constraints, complex mechanisms, membrane clogging, limited flow rates and the production of undesirable by-products.

In this context, adsorption is emerging as one of the most versatile and widely adopted methods in water treatment technologies. Its advantages, such as low cost, superior performance, ease of use, higher yields and simple design, make it a preferred solution (Anastopoulos *et al.*, 2017; Bilal *et al.*, 2020; Pai *et al.*, 2021). However, commercial activated carbons, the main adsorbents used, are relatively expensive, require regeneration, which is a limiting factor, and are not widely accessible to developing countries (Deniz and Yildiz, 2019).

In the search for a harmonious balance between economic growth and environmental protection, an innovative concept has aroused the interest of researchers: that of the sustainable economy (Das *et al.*, 2024). With this in mind, research is increasingly focusing on the exploitation of waste, including agricultural waste, as potential adsorbents that are both environmentally friendly and economically viable for eliminating pollutants (Hoc Thang *et al.*, 2021; Nehra *et al.*, 2020; Demba N'diaye *et al.*, 2022; Saeed *et al.*, 2022).

The fruit of *Saba senegalensis* is in the form of a globular husk measuring around 7 to 10 cm long and 6 to 8 cm wide, containing seeds surrounded by orange-yellow pulp that is very soft, juicy, tangy and sweet. In nutritional terms, studies by Hadja *et al.* (2019) have shown that *Saba Senegalensis* fruit is a genuine source of provitamin A, which plays a significant role in cancer prevention. Furthermore, according to the work of the Salamata *et al.* (2020) team, indigenous fruits present numerous opportunities for adding value, particularly in the form of juice, jam and wine, thereby contributing to nutrition, individual health and improved livelihoods. However, once the seeds have been used, the shells are often left behind, creating waste. Exploiting these hulls as a biosorbent could not only help to treat textile effluent, but also address the problem of waste in our cities.

This is the background to the present study, which aims to optimize the process for preparing a biosorbent derived from *Saba Senegalensis* hulls. The optimization tool used in this study is the experimental design methodology, a powerful technique that is increasingly used to optimize water treatment techniques (Daouda *et al.*, 2021; Kebir *et al.*, 2023; Omwoyo and Otieno, 2024). To do this, a screening of factors was carried out using a Plackett-Burman design. Next, a predictive mathematical model was sought that was perfectly suited to the phenomenon under study. To this end, a first-degree design was first considered using a full factorial design. Then, a composite central design, which leads to a degree 2 polynomial model, was used, if necessary, when the degree 1 model was not suitable. Finally, control tests were carried out to check that the experimental results matched those predicted by the model.

The interest of this study lies in the fact that the *Saba Senegalensis* hulls used in this work have never been used for this type of work before. The other interesting aspect is the modelling of the process of transforming the hulls into a biosorbent, which makes it possible to predict the adsorption capacity of this material as a function of the experimental conditions.

2. Materials and methods

2.1. Preparation of the biosorbent

2.1.1. Collection and pre-treatment of biomass

The *Saba Senegalensis* hulls were collected from fruit sellers in a market in Daloa, a town in the west of Côte d'Ivoire. The hulls were then washed with tap water to remove any impurities. Preparing the biosorbent involved four essential stages: drying, grinding, sieving and washing.

2.1.2. Drying

The material was dried in a Memmert-type oven at various temperatures, the values of which were set by the experimental design. To prevent any alteration in the physicochemical properties of the adsorbent materials, a moderate temperature range was chosen.

2.1.3. Grinding

The dried biomass was crushed to obtain homogeneous particles for the laboratory studies. This operation was carried out in two successive stages: First, the dried biomass was crushed manually. Then, it was introduced into a Retsch SK 100 type knife mill equipped with removable blades for grinding.

2.1.4. Screening

After the grinding stage, the shreds obtained were mechanically isolated using three sieves with mesh sizes set according to the experimental conditions. This range of particle sizes was chosen to ensure good dispersion of the material during the biosorption tests, and to improve the repeatability of the tests.

2.1.5 Washing

Washing was carried out by bringing a mass of crushed material into contact with a quantity of NaOH or H₂SO₄ at concentrations fixed according to the experimental conditions imposed by the design of experiments. The suspension obtained was stirred using a magnetic stirrer (HI 200M) made by Hanna at a speed of 350 rpm for a time and at a temperature defined according to the experimental plans. After washing, the materials obtained were dried again at a given temperature, which varied according to the tests.

2.2 Research into the optimum conditions for preparing the biosorbent

The optimum conditions for the preparation of the biosorbent were obtained using the design of experiments methodology, which is the opposite of the 'one factor at a time' method that consists of varying each factor, one after the other, by assigning all possible values (Tinsson, 2010). Throughout the study, the methylene blue elimination rate is the only response used as an index of material performance.

Firstly, a Plackett-Brumann design (PBD) was used to screen for 6 factors likely to have an influence on the response. These included drying temperature (X1), particle size (X2), type of activating agent (X3), activation time (X4), activating agent concentration (X5) and activation temperature (X6).

In this type of design, all the factors each have two levels: a low level (-) and a high level (+). These levels are numbers in the case of a quantitative factor, and a state in the case of a qualitative factor.

Table 1 below shows the coded and uncoded values of the factors as well as the experimental domain for this design.

Table 1 : Factors and experimental range for the Plackett and Burman design

Coded variables (Xi)	Facteurs	Experimental field	
		Low level (-1)	High level (+1)
X1	Drying temperature (°C)	40	80
X2	Particle size	φ_1	φ_2
X3	Type of activating agent	H ₂ SO ₄	NaOH
X4	Activation time (h)	2	4
X5	Activating agent concentration (N)	0.1	0.5
X6	Activation temperature (°C)	26	70

In this table φ_1 represents particle sizes between 0.2mm and 0.5mm and φ_2 those between 0.5mm and 1mm.

The mathematical model linking the response ER (elimination rate) and the factors Xi is a first-degree model without interactions given by the relationship below (Eqn. 1):

$$ER = a_0 + \sum_{i=1}^6 a_i X_i \quad \text{Eqn. 1}$$

In this relationship a_0 represents the constant (or average effect) of the model and a_i the effects of the factors. These effects make it possible to judge whether a factor Xi has a significant influence or not.

A full factorial design (FFD) was then used to find a first-degree model to explain the phenomenon involved. For k factors, this design is called representing the number of trials required to determine the coefficients of the effects of the factors. The degree 1 polynomial model of the FFD used in this study is given by Eqn. 4

$$ER_1 = a_0 + \sum_{i=1}^k a_i x_i + \sum_{ij} a_{ij} x_i x_j \quad \text{Eqn. 4}$$

In this model, the coefficients a_{ij} represent the effects of second-order interactions between factors.

Finally, a central composite design (CCD) was used to model the phenomenon and determine the optimal conditions using the response surface methodology. This design is made up of three parts: a complete two-level factorial design 2^k , where k represents the number of factors, a star design n_0 and one of the tests in the centre of the domain.

The mathematical model resulting from this plan is a polynomial of degree 2 given by Eqn. 5

$$ER_2 = a_0 + \sum a_i X_i + \sum a_{ij} X_i X_j + \sum a_{ii} X_i^2 \quad \text{Eqn. 5}$$

In this model, the a_{ii} represent the quadratic terms.

Minitab 19 was used to set up the experimental designs, calculate the coefficients and determine the statistical values for the various experimental designs.

2.3 Methods for evaluating coefficients and validating models

There are several criteria for judging the validity of models and their experimental design coefficients. In this study, the factor coefficients and significance of the models were assessed using multiple regression analysis and ANOVA.

Model terms were retained or discarded according to the P value, with a confidence level of 95% ($p < 0.05$). The significance of the models was first assessed by comparing the regression mean square with

the residual mean square. According to [Bezerra et al. \(2019\)](#), a fit is considered adequate if the sum of squares due to the residuals (errors) is less than one-third of the sum of squares due to the model. Also, the sum of squares due to the pure error was compared to the total sum of squares ([Tinsson, 2010](#)). The quality of the models was also assessed using the coefficients of determination R^2 and adjusted R^2 , and their statistical significance was verified using Fisher's F test ([Maataoui et al., 2024](#)). Finally, these results were confirmed by analyzing the coefficient of variation C_V given by the equation below ([Eqn. 6](#)):

$$C_V = \frac{1}{n} \left[\sum_{i=1}^n \left| \frac{ER_{exp} - ER_{cal}}{ER_{exp}} \right| \right] \times 100 \quad \text{Eqn. 6}$$

In this relationship, n denotes the number of tests carried out, ER_{exp} and ER_{cal} represent the experimental and model-calculated elimination rates respectively.

Furthermore, it is accepted that a model is considered relevant if the coefficient of variation is less than 5%. ([Ncibi et al., 2008](#)).

Optimal activation conditions are found using iso-response curves or response surface curves given by the Minitab 19 software. The optimal values of the selected variables were determined using the desirability function available in Minitab, as well as by analyzing the response surface contours.

2.4 Method for assessing the elimination rate of methylene blue

The methylene blue elimination rates of the prepared materials were determined by adsorption tests. These adsorption tests were carried out in batch mode, by bringing 0.2 g of material into contact with 100 ml of a 50 mg/l methylene blue solution in a 250 ml Erlenmeyer flask. The mixture was then stirred for 1 h using a magnetic stirrer at room temperature at a speed of 300 rpm. The coloured solution was separated from the adsorbent by centrifugation at 400 rpm for 12 min. The suspension obtained was analyzed by UV-Visible spectrophotometry at a wavelength of 665 nm to determine the residual concentration. The removal rate is given by the following relationship ([Eqn. 7](#)) ([Parlayıcı and Pehlivan, 2021](#)):

$$ER = \frac{(C_0 - C_e)}{C_0} \times 100 \quad \text{Eqn. 7}$$

T: methylene blue elimination rate (%)

C_0 : initial concentration of methylene blue (in mg/l)

C_e : residual concentration of methylene blue (in mg/l)

3. Results and discussion

3.1 Plackett-Burmann screening design

The results of the Plackett-Burman matrix are given in [Table 2](#) below. The response ER is given by the mean of the two repetitions plus or minus the standard deviation. Analysis of [Table 2](#) reveals that the methylene blue removal rate on biosorbents prepared by the Plackett-Burman design ranged from $27.06 \pm 2.33\%$ to $88.75 \pm 4.03\%$, i.e. a difference of 61.69% in the experimental range. This difference between the minimum and maximum response values shows that preparation conditions have an influence on biosorbent performance ([Mahunon, 2019](#)). Analysis of this table also shows that of the 6 trials involving the use of NaOH, only trials 1 and 8 led to removal rates of over 50%. However, all the trials using sulphuric acid as the activating agent resulted in removal rates of over 60%. It is therefore

clear that treating *Saba Senegalensis* hulls with H₂SO₄ results in more effective biosorbents than those treated with NaOH. Statistical data from the screening of factors for the preparation of biosorbents from *Saba Senegalensis* hulls are given in **Table 3** below.

Table 2: Plackett-Bruman experimental design

Tests	X1	X2	X3	X4	X5	X6	ER (%)
1	60	φ_1	NaOH	2	0.1	26	79.32± 1,36
2	60	φ_2	H ₂ SO ₄	4	0.1	26	72.25± 0,75
3	35	φ_2	NaOH	2	0.5	26	40.83± 1,11
4	60	φ_1	NaOH	4	0.1	50	27.06± 2,33
5	60	φ_2	H ₂ SO ₄	4	0.5	26	80.11± 5,81
6	60	φ_2	NaOH	2	0.5	50	31.37± 7,32
7	35	φ_2	NaOH	4	0.1	50	31.53± 7,31
8	35	φ_1	NaOH	4	0.5	26	58.14± 1,06
9	35	φ_1	H ₂ SO ₄	4	0.5	50	73.48± 25,42
10	60	φ_1	H ₂ SO ₄	2	0.5	50	88.75± 4,03
11	35	φ_2	H ₂ SO ₄	2	0.1	50	61.63± 0,02
12	35	φ_1	H ₂ SO ₄	2	0.1	26	86.20± 6,37

Table 3: Statistical analysis of coefficients

Factor	(X1)	(X2)	(X3)	(X4)	(X5)	(X6)
Coefficients	4.51	-15.87	-32.36	-7.59	2.45	-17.17
P-value	0.34	0.003	0.000	0.120	0.604	0.002

According to the results of the table above, 3 factors have a significant influence on the rate of BM elimination among the 6 factors studied for the screening, their p values being less than 0.05. These factors are in hierarchical order: type of activating agent, drying temperature and particle size.

The type of activating agent (X3) was the most influential factor in this screening, with a zero p-value. The negative coefficient of this factor indicates that the low level of its domain is the most appropriate for obtaining high BM elimination rates. This low level corresponds to the use of sulphuric acid as an activating agent. This result supports the observation in the previous paragraph that all the tests using sulphuric acid as the activating agent resulted in BM removal rates of over 60%.

The negative coefficients for drying temperature (X6) and particle size (X2) indicate that the most effective particles are those between 0.2 mm and 0.5 treated at ambient temperature. This result confirms the idea that in batch mode, small particles are the most favourable for adsorbing pollutants (Alwared *et al.*, 2021; Liu *et al.*, 2012). These particles generally have a higher specific surface area, which facilitates biosorption processes and shortens the equilibrium time. However, Park *et al.* (2010) have stated that for dynamic processes such as column adsorption, small particles are not recommended due to their low mechanical strength and the risk of clogging the column.

For factors with insignificant effects such as drying temperature (X1), treatment time (X4), and activating agent concentration (X5), only the X1 factor was fixed in the rest of the study. The type of activating agent and granulometry are qualitative factors. In addition, it is not technically possible to use treatment temperatures below ambient temperature.

The new experimental area and the factors studied for modelling biosorbent performance are described below.

3.2 First-degree model: full factorial design (FFD)

The new experimental area comprises eight tests (2^3). The sulphuric acid concentration, now designated X1, has a low level of 0.5 N and a high level of 2.5 N. This new range for the acid concentration is justified by its positive coefficient in Table 2. In the same way, this approach made it possible to define the new domain of the activation time, noted here (X2) whose low and high levels are 3 h and 6 h respectively. The third factor of this PFC is the impregnation ratio noted here (X3), which is the ratio between the mass of acid and the mass of biomass and whose low and high levels are 5 and 10 respectively.

The results of the eight (8) FFD tests carried out are shown in **Figure 1** below, where ER (%) is the methylene blue elimination rate in this first-degree model.

According to this figure, the elimination rate varies between 52.07%, a response measured in test number 2, and 93.92%, which is a response measured in the seventh test. It should be noted that the minimum value of the responses obtained in this PFC is practically double that obtained in the case of the screening plan, which shows an improvement in the quality of the biosorbent.

In addition, the results of the descriptive statistics on the responses using SPSS software indicate that the mean and median values of the responses are 64.3% and 62.5% respectively. These more or less similar values show a relatively symmetrical distribution of responses around the mean ([Mahunon, 2019](#)).

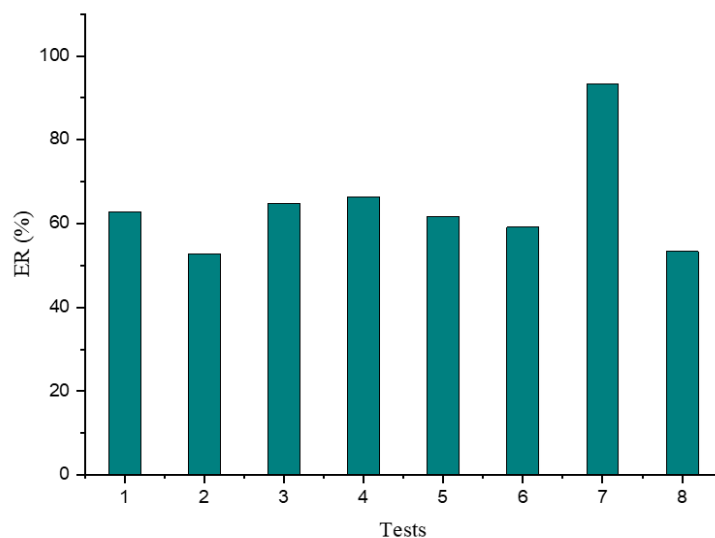


Figure 1. Results of the full factorial design

The first-degree model of the PFC given by the Minitab software is represented by the equation below, where ER_1 represents the theoretical elimination rate (**Eqn. 8**)

$$ER_1 = 64.21 - 6.37X_1 + 5.18X_2 + 2.57X_3 - 3.20X_1X_2 - 4.22X_1X_3 + 1.26X_2X_3 \quad \text{Eqn. 8}$$

Table 4 below shows the results of the analysis of variance (ANOVA) of the full factorial design.

Table 4: Analysis of variance for the full factorial design

Sources of variance	DF	Sum of squares	Medium squares	F-value	P-value
Model	6	878.88	146.48	3.72	0.015
Error	17	669.10	39.359		
Inadequate fit	1	2.51	2.507	0.06	0.809
Pure error	16	666.59	41.662		
Total	23	1547.98			
R ²	56.78 %				
R _A ²	41.52 %				

According to the results of the analysis of variance (ANOVA) presented in **Table 4**, the probability of significance, expressed by the p-value, is less than 0.05. However, by examining the other data in this table, it appears that this first-degree model cannot be validated (Adjoumani *et al.*, 2019; Omwoyo and Otieno, 2024). Indeed, the sum of the squares of the residuals, amounting to 669.10, is not less than a third of the sum of the squares of the model, which is 878.88. In addition, the coefficients of determination R_A^2 and R_A^2 show values of 56.78% and 41.52% respectively, indicating an insufficient correlation between the experimental data and those predicted by the model (Rittisak *et al.*, 2023). Consequently, it was deemed necessary to opt for a second-degree model using a response surface design. But before doing so, it is imperative to understand the degree of influence of each factor and interaction. This degree of influence is illustrated by the Pareto diagram shown in **Figure 2** below.

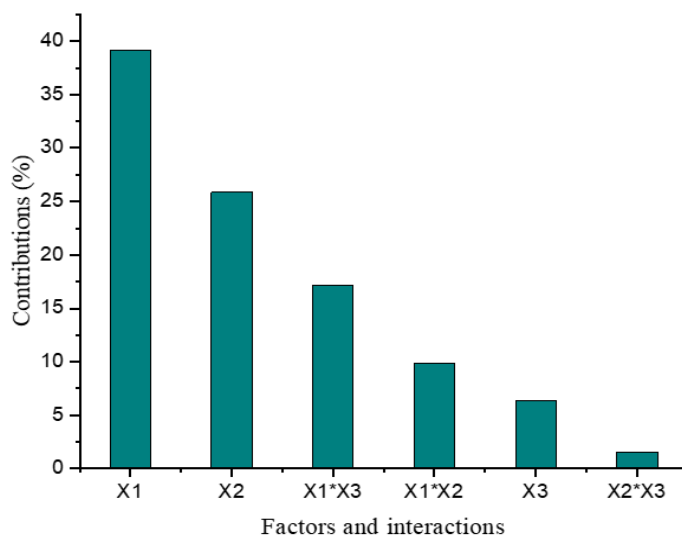
**Figure 2.** Pareto chart showing the contributions of the three factors and their interactions

Figure 2 shows that over 80% of the variation in response is explained by sulphuric acid concentration (X1), activation time (X2) and the interaction between acid concentration and ratio (X1*X3). The most influential factor was sulphuric acid concentration, with a contribution of 39.2%. Next came the activation time and the ratio, with contributions of 25.9% and 17.2% respectively. The contributions of the ratio (X3), the interaction between concentration and activation time (X1*X2) and the interaction between activation time and ratio (X2*X3) were all less than 10%.

The main effects diagram that follows (**Figure 3**) illustrates how each level of the factors affects adsorption capacity. By analyzing this diagram, we aim not only to understand the general direction

and intensity of the effect of each factor, but also to identify the levels that produce the most optimal results.

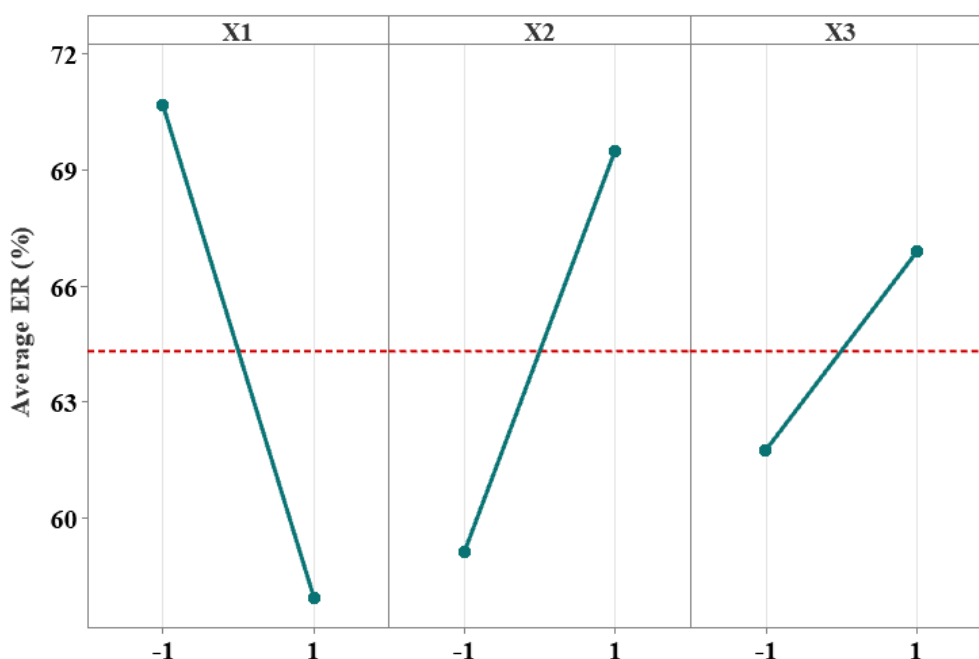


Figure 3. Diagram of the main effects of the factors

Figure 3 shows that the rate of methylene blue elimination decreases as the concentration of sulphuric acid (X1) increases. In fact, the elimination rate decreases on average from 70.6% to 57.9% when the acid concentration increases from 0.5 N to 2.5 N, which corresponds to a 12.7% reduction in biosorbent performance. Thus, an increase in the concentration of sulphuric acid has an unfavorable impact on the efficiency of the biosorbent. On the other hand, extending the treatment time (X2) had a positive influence on the response. The elimination rate increased on average from 59.13% to 69.48% when the activation time was increased from 3 h to 6 h.

Furthermore, analysis of the Pareto chart (**Figure 2**) revealed that the ratio (X3) did not exert a statistically significant influence on the response. Nevertheless, examination of **Figure 2** indicates that preparing the biosorbent with the high level of this factor improves the elimination rate. Thus, in the rest of the study, the biomasses were impregnated with a ratio of 10.

Since the degree of involvement, general direction and intensity of effect of each factor and interaction are known, the results of the second-order model adopted for modelling and optimizing the response are presented below.

3.3 Response surface plane: two-factor central composite design

The central composite design (CCD) was developed using two factors ($k = 2$) the sulphuric acid concentration (X1) and the activation time (X2).

This plan is made up of three parts and involves a total of 13 tests:

- four trials resulting from a full factorial design (2^2)
- four star tests $2 \times k$
- five trials at the center of the estate

The domain of each factor is therefore between $-\alpha$ and $+\alpha$ equal to $2^{k/4}$ i.e. between -1.414 and +1.414. In real terms, the sulphuric acid concentration is between 1 N and 2 N and the activation time is between 4h and 8h.

The experimental results of the PCC (ER_2 exp), the predictive responses of the model (ER_2 cal) and the coefficients of variation are shown in **Table 5** below. Trials 1 to 4 are from the full factorial design (2^2), trials 5 to 8 are from the star design and trials 9 to 13 are from the center of the domain.

Table 5: Matrix, experimental design, elimination rates and coefficients of variation for the central composite design

Tests	X1	X2	ER ₂ exp	ER ₂ cal	Residues	Coefficient variation	of
1	-1	-1	90.08	90.46	-0.39	0.43	
2	1	-1	82.34	81.88	0.46	0.56	
3	-1	1	93.40	93.13	0.27	0.29	
4	1	1	86.42	85.29	1.12	1.30	
5	-1.414	0	95.95	95.72	0.24	0.25	
6	1.414	0	83.14	84.11	-0.97	1.16	
7	0	-1.414	83.42	83.32	0.10	0.12	
8	0	1.414	86.79	87.62	-0.83	0.96	
9	0	0	83.10	83.30	-0.20	0.24	
10	0	0	84.62	83.30	1.33	1.57	
11	0	0	82.77	83.30	-0.52	0.63	
12	0	0	83.75	83.30	0.46	0.54	
13	0	0	82.23	83.30	-106	1.29	

The results in **Table 5** show that there is an overall improvement in the methylene blue elimination rate under the experimental conditions, with the minimum value of the experimental responses being greater than 80%.

The differences between the measured responses and the responses calculated by the model (Residuals) are all less than 2 in absolute value.

The second-degree model resulting from this PCC is represented by the equation below where ER_2 represents the theoretical elimination rate (**Eqn. 9**)

$$ER_2 = 83,29 - 4,1X_1 + 1,55X_2 + 3,3X_1^2 + 1,08X_2^2 + 1,08X_1X_2 \quad \text{Eqn. 9}$$

The coefficients of this model are the effects of the factors and their interactions.

The statistical data used to evaluate this model are presented in **Table 6** of the analysis of variance (ANOVA) below:

Table 6: Analysis of variance for the central composite design

Sources of variance	DF	Sum of squares	Medium squares	F-value	P-value
Model	5	232.667	46.533	47.83	0.000
Error	7	6.810	0.973		
Inadequate fit	3	3.397	1.132	1.33	0.383
Pure error	4	3.413	3.413		
Total	12	239.476	239.476		
R ²	97.16 %				
R _A ²	95.13 %				
Cv	0.72 %				

This table indicates that, according to the validity criteria of (Oelofse *et al.*, 2023), the sum of the squares of the residuals, which has a value of 6.810, is much lower than the sum of the squares of the regression, which is 232.667. Furthermore, the probability of significance of the model, expressed by the p-value, is zero, indicating that the main effect of the regression is highly significant. The table also shows that the sum of squares due to purely experimental error has a value of 3.413, corresponding to a contribution of only 1.42% of the total sum of squares. It therefore appears that these errors can be neglected (Suditu *et al.*, 2022).

Furthermore, the coefficients of determination R² and R_A² are greater than 80% and 77% respectively. This shows a good match between the experimental values and those given by the second-degree model above. Finally, the average coefficient of variation (Cv) was well below 5%. All these data show that the second-order model postulated above is suitable for describing the phenomenon studied (Oelofse *et al.*, 2023; Omwoyo and Otieno, 2024; Suditu *et al.*, 2022).

3.4 Optimisation of the methylene blue elimination rate

The optimization method used was based on the isoresponse diagram shown in **Figure 4** below. Analysis of this figure shows that it is possible to achieve elimination rates of even more than 99% while remaining within the field of study. All that needs to be done is to select a sulphuric acid concentration (X1) and an activation time (X2) which, together, give an elimination rate on or above the 99-level line (in red) (see **Figure 4**).

We therefore need to determine the coded values X1 and X2 which are within the experimental range and which satisfy this condition on the answer, ER₂ being described by the second-degree polynomial. The isoresponse diagram for optimizing the methylene blue rate is shown in **Figure 4** below.

Analysis of this figure shows that it is possible to achieve elimination rates of even more than 99% while remaining within the field of study. All you have to do is select a sulphuric acid concentration (X1) and an activation time (X2).

The aim is therefore to determine the coded values X1 and X2 which are within the experimental range and which meet this condition on the response ER₂, which is described by **Eqn. 9**

These values were determined using the desirability function in Minitab software and are presented in **Figure 5** below. The aim of this study is to optimize the capacities of the biosorbent prepared from Saba hulls by maximizing the methylene blue removal rate.

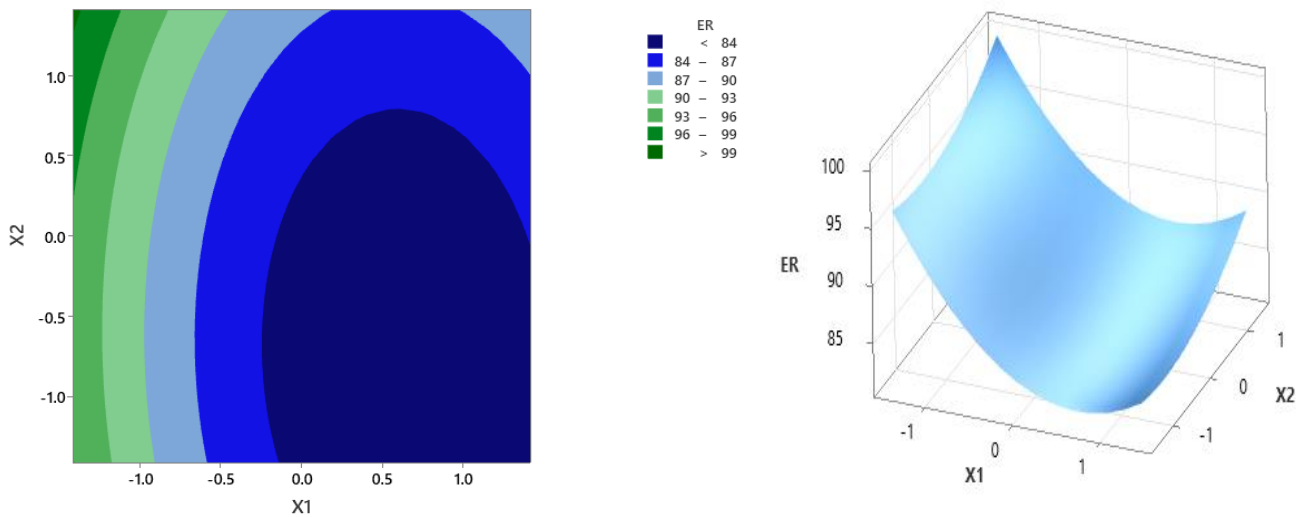


Figure 4 : Contour and response surface diagram

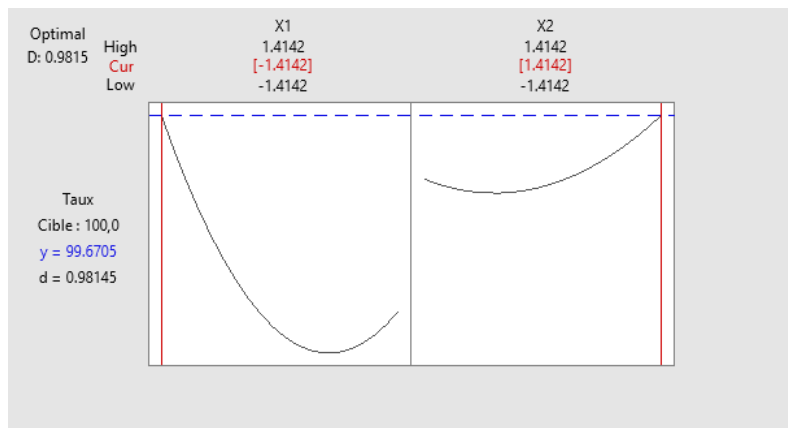


Figure 5: Desirability profile of methylene blue elimination rate

Figure 5 shows that with a desirability of 98.14%, it is possible to remove 99.67% of the methylene blue from the prepared biosorbent. The optimum condition resulting from solving the equation is obtained at a point where the concentration of sulphuric acid and the activation time are -1.414 and 1.414 respectively in coded values. The corresponding real values were determined using the formula for converting coded variables into real variables. In this study, the optimum concentration of sulphuric acid obtained is 1N and the optimum activation time obtained is 8h. Under these conditions, there is a 95% chance that the biosorbent prepared will have a methylene blue removal rate of between 95.5% and 100%.

Once the optimum conditions had been found, additional tests (control tests) were carried out to confirm these results. This table shows that the optimum condition resulting from the solution of the equation is obtained at a point where the concentration of sulphuric acid and the activation time are -1.414 and 1.414 respectively in coded values. The corresponding real values were determined using the formula for converting coded variables into real variables. In this study, the optimum concentration of sulphuric acid obtained is 1N and the optimum activation time obtained is 8h. Under these conditions, there is a 95% chance that the biosorbent prepared will have a methylene blue removal rate of between 95.5% and 100%. The optimum conditions having been found; additional tests (control tests) were carried out to confirm these results.

Table 2. Prediction of responses

Factors	Configurations	
X1	-1.414	
X2	-1.414	
Response	Adjusted value	95% confidence interval
Elimination rate	99.67	(95.5 ; 100)

3.5 Results of the control test

The experimental matrix for the control tests is shown in **Table 7** below.

Table 7: Results of control tests under optimal biosorbent preparation conditions

Tests	Concentration of sulphuric acid (N)	Activation time (h)	ERcal (%)	ERexp (%)	Average elimination rate (%)
14	1	8	99.67	97.23	
15	1	8	99.67	94.78	96.02
16	1	8	99.67	98.06	

Based on the three control tests, the mean elimination rate is 96.02%, with a standard deviation of 1.22. Given that the value predicted by the model is 99.67%, we note a deviation of 3.79%. This parameter, less than 5%, validates the results obtained.

The results obtained in this study are in agreement with recent previous work in the field of biosorption. For example, previous studies such as those by (Coşkun, 2022; Kouadio *et al.*, 2023; Ifguis *et al.*, 2022; Selengil and Yıldız, 2022) reported comparable removal rates using biosorbents from Argania Shells and perlite waste and green walnut shells and cocoa pod shells. It should also be noted that the performance of this biosorbent is comparable to that of activated carbons (Kamdod and Kumar, 2022; Lee *et al.*, 2024). This remarkable efficiency can be attributed to the design-of-experiments methodology used, which made it possible to optimize the adsorption capacities of *Saba senegalensis* (Kebir *et al.*, 2023; Meledje *et al.*, 2024; Omwoyo and Otieno, 2024). In addition, chemical activation of the material by sulphuric acid helped to improve its adsorption capacity.

Conclusion

The aim of this study was to determine the optimum conditions for the preparation of a biosorbent derived from *Saba Senegalensis* hulls using experimental design methodology. Several factors involved in the preparation process were studied, including drying temperature, granulometry, nature of the activating agent, activation time, concentration of the activating agent and activation time. The results of the Plackett-Burman screening showed that the type of activating agent, granulometry and activation

temperature were the most influential factors. The preparation process was modelled with a central composite design using response surfaces and the desirability function generated by Minitab 19 software. The optimum conditions obtained were based on the use of biomass particles of sizes ranging from 0.2 mm to 0.5 mm, activated at room temperature using 1 N sulphuric acid for 8 h. Under these conditions, the methylene blue removal rate was 96.02%.

The use of *Saba senegalensis* hulls as a biosorbent therefore presents an economically viable and sustainable alternative to commercial adsorbents such as activated carbon. With low preparation costs and attractive disposal results, this biosorbent could not only offer an effective solution for wastewater treatment, but also contribute to a more eco-responsible approach to waste management. Further studies on specific costs and cost-benefit analysis would be beneficial to validate these economic advances and strengthen their industrial application.

Disclosure statement: *Conflict of Interest:* The authors declare that there are no conflicts of interest.

Compliance with Ethical Standards: This article does not contain any studies involving human or animal subjects.

References

- Aaddouz M., Azzaoui K., Akartasse N., Mejdoubi E., *et al.* (2023). Removal of Methylene Blue from aqueous solution by adsorption onto hydroxyapatite nanoparticles, *Journal of Molecular Structure*, 1288, 135807, <https://doi.org/10.1016/j.molstruc.2023.135807>
- Adegoke, K. A., & Bello, O. S. (2015). Dye sequestration using agricultural wastes as adsorbents. *Water Resources and Industry*, 12, 8-24. <https://doi.org/10.1016/j.wri.2015.09.002>
- Adjoumani, Y. J., Dablé, P. J. M. R., Kouassi, K. E., Gueu, S., Assémian, A. S., & Yao, K. B. (2019). Modeling and Optimization of Two Clays Acidic Activation for Phosphate Ions Removal in Aqueous Solution by Response Surface Methodology. *Journal of Water Resource and Protection*, 11(02), 200-216. <https://doi.org/10.4236/jwarp.2019.112012>
- Akartasse N., Azzaoui K., Mejdoubi E., *et al.* (2022), Environmental-Friendly Adsorbent Composite Based on Hydroxyapatite/Hydroxypropyl Methyl-Cellulose for Removal of Cationic Dyes from an Aqueous Solution, *Polymers*, 14(11), 2147; <https://doi.org/10.3390/polym14112147>
- Alwared, A. I., Al-Musawi, T. J., Muhaisn, L. F., & Mohammed, A. A. (2021). The biosorption of reactive red dye onto orange peel waste: A study on the isotherm and kinetic processes and sensitivity analysis using the artificial neural network approach. *Environmental Science and Pollution Research*, 28(3), 2848-2859. <https://doi.org/10.1007/s11356-020-10613-6>
- Anastopoulos, I., Karamesouti, M., Mitropoulos, A. C., & Kyzas, G. Z. (2017). A review for coffee adsorbents. *Journal of Molecular Liquids*, 229, 555-565. <https://doi.org/10.1016/j.molliq.2016.12.096>
- Bezerra, M. A., Ferreira, S. L. C., Novaes, C. G., dos Santos, A. M. P., Valasques, G. S., da Mata Cerqueira, U. M. F., & dos Santos Alves, J. P. (2019). Simultaneous optimization of multiple responses and its application in Analytical Chemistry – A review. *Talanta*, 194, 941-959. <https://doi.org/10.1016/j.talanta.2018.10.088>
- Bilal, M., Wang, Z., Cui, J., Ferreira, L. F. R., Bharagava, R. N., & Iqbal, H. M. N. (2020). Environmental impact of lignocellulosic wastes and their effective exploitation as smart carriers – A drive towards greener and eco-friendlier biocatalytic systems. *Science of The Total Environment*, 722, 137903. <https://doi.org/10.1016/j.scitotenv.2020.137903>
- Bilińska, L., & Gmurek, M. (2021). Novel trends in AOPs for textile wastewater treatment. Enhanced dye by-products removal by catalytic and synergistic actions. *Water Resources and Industry*, 26, 100160. <https://doi.org/10.1016/j.wri.2021.100160>

- Chin, S. X., Lau, K. S., Zakaria, S., Chia, C. H., & Wongchoosuk, C. (2022). Chitosan Fibers Loaded with Limonite as a Catalyst for the Decolorization of Methylene Blue via a Persulfate-Based Advanced Oxidation Process. *Polymers*, 14(23), 5165. <https://doi.org/10.3390/polym14235165>
- Coşkun, Y. İ. (2022). Investigation of adsorption performances of green walnut hulls for the removal of methylene blue. *Desalination and Water Treatment*, 247, 281-293. <https://doi.org/10.5004/dwt.2022.28075>
- Daouda, M. M. A., Akowanou, A. V. O., Mahunon, S. E. R., Adjinda, C. K., Aina, M. P., & Drogui, P. (2021). Optimal removal of diclofenac and amoxicillin by activated carbon prepared from coconut shell through response surface methodology. *South African Journal of Chemical Engineering*, 38, 78-89. <https://doi.org/10.1016/j.sajce.2021.08.004>
- Das, K., Sukul, U., Chen, J.-S., Sharma, R. K., Banerjee, P., Dey, G., Taharia, Md., Wijaya, C. J., Lee, C.-I., Wang, S.-L., Nuong, N. H. K., & Chen, C.-Y. (2024). Transformative and sustainable insights of agricultural waste-based adsorbents for water defluoridation : Biosorption dynamics, economic viability, and spent adsorbent management. *Heliyon*, 10(8), e29747. <https://doi.org/10.1016/j.heliyon.2024.e29747>
- David Léonce, K., Yapo Hermann Aristide, Y., Djedjess Essoh Jules-César, M., Kacou Alain Paterné, D., Djamatché Paul Valéry, A., Brou, D., Kouamé Bini, D., & Karim Sory, T. (2023). Contribution to the Modeling of a Biosorbent Derived from Cocoa Pod Shells on the Methylene Blue Index. *American Journal of Applied Chemistry*. <https://doi.org/10.11648/j.ajac.20231102.11>
- Deniz, F., & Yildiz, H. (2019). Taguchi DoE methodology for modeling of synthetic dye biosorption from aqueous effluents: Parametric and phenomenological studies. *International Journal of Phytoremediation*, 21(11), 1065-1071. <https://doi.org/10.1080/15226514.2019.1594687>
- Hadja Mawa Fatim, D., Souleymane, T., Mohamed, C., Doudjo, S., & Kouakou, B. (2019). Biochemical Characterization and Nutritional Profile of the Pulp of *Saba senegalensis* from Côte d'Ivoire Forest. *American Journal of Food and Nutrition*, 7(1), 19-25. <https://doi.org/10.12691/ajfn-7-1-4>
- Hasanpour, M., & Hatami, M. (2020). Photocatalytic performance of aerogels for organic dyes removal from wastewaters: Review study. *Journal of Molecular Liquids*, 309, 113094. <https://doi.org/10.1016/j.molliq.2020.113094>
- Hassan, M., Naidu, R., Du, J., Liu, Y., & Qi, F. (2020). Critical review of magnetic biosorbents: Their preparation, application, and regeneration for wastewater treatment. *Science of The Total Environment*, 702, 134893. <https://doi.org/10.1016/j.scitotenv.2019.134893>
- Hoc Thang, N., Sy Khang, D., Duy Hai, T., Thi Nga, D., & Dinh Tuan, P. (2021). Methylene blue adsorption mechanism of activated carbon synthesised from cashew nut shells. *RSC Advances*, 11(43), 26563-26570. <https://doi.org/10.1039/D1RA04672A>
- Ifguis, O., Ziat, Y., Ammou, F., Bouhdadi, R., Mbarki, M., & Benchagra, M. (2022). Theoretical and experimental study on the thermodynamic parameters and adsorption of methylene blue on "Argania shells" in industrial waters. *South African Journal of Chemical Engineering*, 41, 211-222. <https://doi.org/10.1016/j.sajce.2022.06.010>
- Jaafar A., Boussaoud A., Azzaoui K., Mejdoubi E., et al. (2016), Decolorization of Basic Red 5 in aqueous solution by Advanced Oxidation Process using Fenton's reagent, *Mor. J. Chem.* 4, 759-763, <https://doi.org/10.48317/IMIST.PRSM/morjchem-v4i3.5206>
- Kamdod, A. S., & Pavan Kumar, M. V. (2022). Adsorption of Methylene blue and Methyl orange on tamarind seed activated carbon and its composite with chitosan: Equilibrium and kinetic studies. *Desalination and Water Treatment*, 252, 408-419. <https://doi.org/10.5004/dwt.2022.28270>
- Katheresan, V., Kansedo, J., & Lau, S. Y. (2018). Efficiency of various recent wastewater dye removal methods: A review. *Journal of Environmental Chemical Engineering*, 6(4), 4676-4697. <https://doi.org/10.1016/j.jece.2018.06.060>

- Kebir, M., Benramdhan, I.-K., Nasrallah, N., Tahraoui, H., Bait, N., Benaissa, H., Ameraoui, R., Zhang, J., Assadi, A. A., Mouni, L., & Amrane, A. (2023). Surface response modeling of homogeneous photo Fenton Fe (III) and Fe (II) complex for sunlight degradation and mineralization of food dye. *Catalysis Communications*, 183, 106780. <https://doi.org/10.1016/j.catcom.2023.106780>
- Khamparia, S., & Jaspal, D. K. (2017). Adsorption in combination with ozonation for the treatment of textile waste water: A critical review. *Frontiers of Environmental Science & Engineering*, 11(1), 8. <https://doi.org/10.1007/s11783-017-0899-5>
- Lee, H., Fiore, S., & Berruti, F. (2024). Adsorption of methyl orange and methylene blue on activated biocarbon derived from birchwood pellets. *Biomass and Bioenergy*, 191, 107446. <https://doi.org/10.1016/j.biombioe.2024.107446>
- Liu, C., Ngo, H. H., Guo, W., & Tung, K.-L. (2012). Optimal conditions for preparation of banana peels, sugarcane bagasse and watermelon rind in removing copper from water. *Bioresource Technology*, 119, 349-354. <https://doi.org/10.1016/j.biortech.2012.06.004>
- Maataoui, Y. E., Alehyen, S., Fadil, M., Aouan, B., Liba, A., Saufi, H., & Taibi, M. (2024). Application of Central Composite Design for Optimizing Mechanical Performance of Geopolymer Paste from Fly Ash Using the Mechanochemical Synthesis Method: Structural and Microstructural Analysis. *Iranian Journal of Science and Technology, Transactions of Civil Engineering*. <https://doi.org/10.1007/s40996-024-01601-8>
- Mahunon, S. E. R. (2019). *Optimisation de l'élimination de la pollution organique et métallique des eaux usées par lagunage à Eichhornia crassipes*. Institut national polytechnique Felix Houphouët-Boigny.
- Meledje, D. E. J. C., Yapi, Y. H. A., Kouadio, D. L., Akesse, D. P. V., & Yeo, K. (2024). Optimized Adsorption of Small and Medium Molecules by a Biosorbent Based on Hevea Hulls. *Journal of Materials Science and Chemical Engineering*, 12(09), 69-83. <https://doi.org/10.4236/msce.2024.129004>
- Moradihamedani, P. (2022). Recent advances in dye removal from wastewater by membrane technology: A review. *Polymer Bulletin*, 79(4), 2603-2631. <https://doi.org/10.1007/s00289-021-03603-2>
- Demba N'diaye A., Hammouti B., Nandiyanto A. B. D., Al Husaeni D. F. (2022), A review of biomaterial as an adsorbent: From the bibliometric literature review, the definition of dyes and adsorbent, the adsorption phenomena and isotherm models, factors affecting the adsorption process, to the use of Typha species waste as a low-cost adsorbent, *Communications in Science and Technology*, 7 No.1, 140-153
- Ncibi, M. C., Mahjoub, B., & Seffen, M. (2008). Étude de la biosorption du chrome (VI) par une biomasse méditerranéenne : *Posidonia oceanica* (L.) delile. *Revue des sciences de l'eau*, 21(4), 441-449. <https://doi.org/10.7202/019166ar>
- Nehra, S., Raghav, S., & Kumar, D. (2020). Biomaterial functionalized cerium nanocomposite for removal of fluoride using central composite design optimization study. *Environmental Pollution*, 258, 113773. <https://doi.org/10.1016/j.envpol.2019.113773>
- Oelofse, M., Rack, R., Hilden, M., & Langguth, P. (2023). Optimization of product characteristics of porous carbon agglomerates using a design of experiments in fluidized bed agglomeration. *Particuology*, S1674200123002845. <https://doi.org/10.1016/j.partic.2023.10.017>
- Omwoyo, F. O., & Otieno, G. (2024). Optimization of Methylene Blue Dye Adsorption onto Coconut Husk Cellulose Using Response Surface Methodology: Adsorption Kinetics, Isotherms and Reusability Studies. *Journal of Materials Science and Chemical Engineering*, 12(02), 1-18. <https://doi.org/10.4236/msce.2024.122001>
- Pai, S., Kini, M. S., & Selvaraj, R. (2021). A review on adsorptive removal of dyes from wastewater by hydroxyapatite nanocomposites. *Environmental Science and Pollution Research*, 28(10), 11835-11849. <https://doi.org/10.1007/s11356-019-07319-9>

- Park, D., Yun, Y.-S., & Park, J. M. (2010). The past, present, and future trends of biosorption. *Biotechnology and Bioprocess Engineering*, 15(1), 86-102. <https://doi.org/10.1007/s12257-009-0199-4>
- Parlayıcı, Ş., & Pehlivan, E. (2021). Biosorption of methylene blue and malachite green on biodegradable magnetic *Cortaderia selloana* flower spikes: Modeling and equilibrium study. *International Journal of Phytoremediation*, 23(1), 26-40. <https://doi.org/10.1080/15226514.2020.1788502>
- Ramutshatsha-Makhwedzha, D., Mavhungu, A., Moropeng, M. L., & Mbaya, R. (2022). Activated carbon derived from waste orange and lemon peels for the adsorption of methyl orange and methylene blue dyes from wastewater. *Heliyon*, 8(8), e09930. <https://doi.org/10.1016/j.heliyon.2022.e09930>
- Rittisak, S., Dechewa, P., Savedboworn, W., & Phungamngoen, C. (2023). Application of the Plackett-Burman design for screening and optimisation of factors affecting the aqueous extract for total anthocyanin content of broken riceberry rice. *International Food Research Journal*, 30(3), 649-655. <https://doi.org/10.47836/ifrj.30.3.09>
- Saeed, M., Muneer, M., Haq, A. U., & Akram, N. (2022). Photocatalysis: An effective tool for photodegradation of dyes—a review. *Environmental Science and Pollution Research*, 29(1), 293-311. <https://doi.org/10.1007/s11356-021-16389-7>
- Salamata, T., Leguet, G., Clarisse, S. C., Fidèle, W. T., & Mamoudou, H. D. (2020). Biochemical composition of Saba senegalensis fruits from Burkina Faso. *African Journal of Food Science*, 14(10), 322-329. <https://doi.org/10.5897/AJFS2020.1992>
- Selengil, U., & Yıldız, D. (2022). Investigation of the methylene blue adsorption onto waste perlite. *Desalination and Water Treatment*, 262, 235-247. <https://doi.org/10.5004/dwt.2022.28530>
- Shelke, B. N., Jopale, M. K., & Katgaonkar, A. H. (2022). Exploration of biomass waste as low-cost adsorbents for removal of methylene blue dye: A review. *Journal of the Indian Chemical Society*, 99(7), 100530. <https://doi.org/10.1016/j.jics.2022.100530>
- Suditu, G. D., Blaga, A. C., Tataru-Farmus, R.-E., Zaharia, C., & Suteu, D. (2022). Statistical Analysis and Optimization of the Brilliant Red HE-3B Dye Biosorption onto a Biosorbent Based on Residual Biomass. *Materials*, 15(20), 7180. <https://doi.org/10.3390/ma15207180>
- Thakur, S., & Chauhan, M. S. (2018). Treatment of Dye Wastewater from Textile Industry by Electrocoagulation and Fenton Oxidation: A Review. In V. P. Singh, S. Yadav, & R. N. Yadava (Éds.), *Water Quality Management* (Vol. 79, p. 117-129). Springer Singapore. https://doi.org/10.1007/978-981-10-5795-3_11
- Tinsson, W. (2010). *Plans d'expérience : Constructions et analyses statistiques*. Springer.
- Verma, A. K., Dash, R. R., & Bhunia, P. (2012). A review on chemical coagulation/flocculation technologies for removal of colour from textile wastewaters. *Journal of Environmental Management*, 93(1), 154-168. <https://doi.org/10.1016/j.jenvman.2011.09.012>

(2025) ; <http://www.jmaterenvirosci.com>